*Progress In Electromagnetics Research, PIER 33, 45–68, 2001*

# PROBABILISTIC RESPONSE OF A TRANSMISSION LINE IN A DISSIPATIVE MEDIUM EXCITED BY AN OBLIQUE PLANE WAVE

**P. T. Trakadas, P. J. Papakanellos, and C. N. Capsalis**

National Technical University of Athens
Department of Electrical and Computer Engineering
Division of Information Transmission Systems
and Material Technology
Iroon Polytechniou 9, Str., Athens, Greece

**Abstract**—In this paper a statistical model of the excitation of a conjugate-matched two-wire transmission line in a lossy half space by an electromagnetic (EM) wave is developed. The EM field, radiating in the air, is obliquely incident to the interface defined by the lossy medium and air. Three different orientations of the transmission line for horizontal and vertical polarization of the EM field are examined. The objective is to derive analytic formulas for the probability density function (pdf) and cumulative distribution function (cdf) of the induced near-end and far-end voltage magnitudes in each case, taking into consideration the statistical behavior of the amplitude of the incident electric field vector and the angle of incidence as well. Consequently, the mean values as well as the typical deviation values are presented and the contribution of each one of the parameters is discussed in detail. Finally, a chi-square goodness-of-fit test is applied in order to fit the distribution of the induced voltage with one of the known distributions.

## Appendix B.

## References

## 1. INTRODUCTION

Electromagnetic interference (EMI) at a transmission line (TL), caused by an electromagnetic (EM) field, is one of the most important issues in EMC studies. In the past, many researchers examined this phenomenon. In [1], C. D. Taylor et al. determined the impedance load currents of a terminated two-wire TL excited by a non-uniform EM field. Later on, A. Smith [2] derived more convenient forms of these currents. In [3, 4] the induced currents in a two-wire TL comprised of a conductor and a rocket are presented. In [5], the worst case solution in matrix notation for the currents in a multi-conductor TL is introduced taking into account the contribution of the mutual coupling. In [6], analytic expressions are given, in both the time and frequency domains, in order to evaluate the near-end voltage of the TL, in free space, for many different cases. Also, in [7] the analytic formulation is presented in order to evaluate, exactly, the currents induced in an insulated cable buried in a lossy half-space.

This paper formulates the voltage induced in a terminated two-wire TL located in a lossy medium due to a uniform plane wave propagating in a homogeneous half-space. Three of the frequently met placements of the TL, in practical cases, are examined for parallel and perpendicular polarization of the plane wave. Due to the finite value of the conductivity, the transmitted EM wave is no longer uniform in the lossy medium.

During the last decade, many scientists investigated the statistical characterization of several phenomena related to EMC studies, such as TL coupling ([8], [16–20]). In the case of a TL excited by an external EM wave, the statistical nature of the problem arises from the fact that in many real cases, some of the parameters influencing the problem are randomly moving or characterized by a statistical behavior. As an example, we can report the case of an embedded TL excited by an EM wave, emitted by an antenna of a hand-held phone, radiating in the far-field region. Due to the relative movement of the TL, in accordance with the position of the radiator, the amplitude of electric field strength, as well as the angle of incidence can be handled as being random variables. In Section 2, three different cases are examined and analytic expressions are given for the voltage induced in the TL. In Section 3 the probabilistic analysis of the problem is presented and discussed. In Section 4 numerical results are given for typical

configuration values and finally chi-square goodness-of-fit test results are illustrated.

## 2. EVALUATION OF THE INDUCED VOLTAGE AT THE TRANSMISSION LINE

The homogeneous half-space where the electromagnetic wave propagates (Region 1) is characterized by the permittivity and permeability of free space ($\varepsilon_1 = \varepsilon_0,\ \mu_1 = \mu_0$). The second half-space region (Region 2) where the transmission line is placed, is characterized by $\varepsilon_2,\ \mu_2 = \mu_0$, and the conductivity of the medium is denoted as $\sigma_2$. The distance of separation between the interface and the lower conductor of the transmission line, for all three cases, is equal to $x_1$. The termination loads are denoted as $R_S,\ R_L$. The following development is based on the transmission time approximation (transverse dimensions $\ll \lambda$). The time dependence assumed in the following development is $\exp(j\omega t)$. In the next paragraphs we develop the deterministic analysis of each one of the particular cases, using the system of partial integro-differential equations introduced by C. D. Taylor et al. in [1]. However, there are several models published in the literature, equivalent or not to the one used in this paper. In [9], three equivalent formulations governing the coupling phenomenon are discussed, namely:

1. Taylor et al. formulation,
2. Agrawal et al. formulation, and
3. Rachidi formulation.

The difference among these formulations lies essentially in the representation of the source terms. In the formulation presented by Taylor et al. the source terms are functions of both electric and magnetic excitation fields. In the formulation introduced by Agrawal et al., the source terms involve only the electric field components. Finally, in the formulation presented by Rachidi, the source terms are solely functions of the magnetic field components. In addition to the aforementioned ones, two more models, commonly used in calculating the lightning induced voltages in power lines are:

- The Rusck model [10], and
- The Chowdhuri-Gross model [11].

These two models are deemed as special cases of the more general and accurate model introduced by Agrawal et al. According to the previous notation, the model used in this paper to calculate the induced voltage is the proper one, although a limitation to the model lies in the lack of inclusion of the common mode current contribution on the TL.

*Case 1 (par)*
Consider a three dimensional Cartesian coordinate system, where $y'$-$z'$ plane is the interface of the two regions, and another Cartesian system, parallel to the first one, whose $x$-axis is identical to $x'$-axis. The electric field vector of EM wave has parallel polarization. The TL is placed at $x$-$z$ plane and the direction of the wave traveling into region 2 is at $x'$-$z'$ plane as shown in Figure 1a.

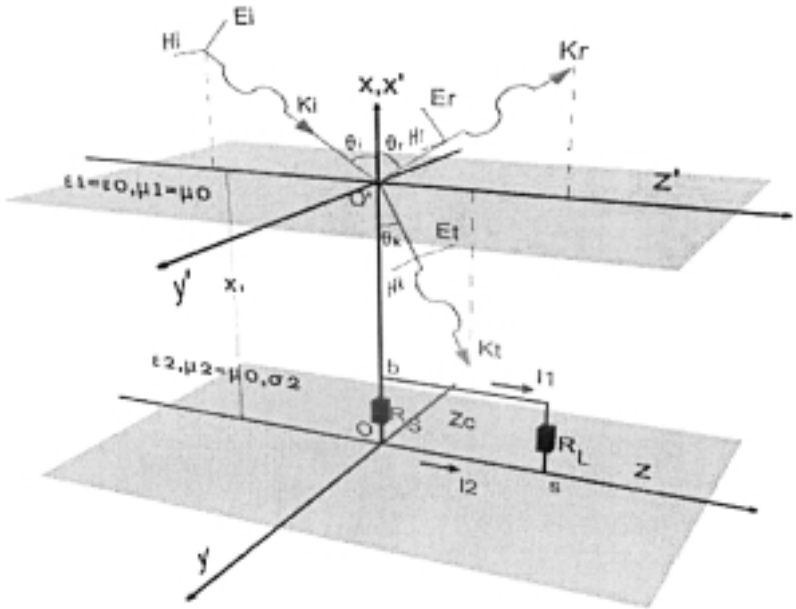


**Figure 1a.** Geometry of Case 1 (par).

The angle of incidence is denoted as $\theta_i$ and the transmission angle as $\theta_t$. The determination of the transmitted EM wave into region 2 is facilitated by solving the wave equation in each region and then satisfying the boundary conditions at the interface ($x' = 0$ plane). The continuity of $E_Z$ component yields [12]:

$$\vec{E}^t = \vec{E}_0^t \cdot \exp\left(-\gamma_2 \cdot (\sin\theta_t \cdot z - \cos\theta_t \cdot x')\right) \tag{1a}$$

$$T_{//} = \left(\frac{E_o^t}{E_o^i}\right)_{//} = \frac{2\gamma_1\gamma_2\cos\theta_i}{\gamma_2^2\cos\theta_i + \gamma_1\sqrt{\gamma_2^2 - \gamma_1^2\sin^2\theta_i}} \tag{1b}$$

where:

$$\gamma_1 = i \cdot \beta_1, \qquad \gamma_2 = \alpha_2 + i \cdot \beta_2$$

are the propagation constants (the definition of propagation constant is given in Appendix A). In order to express the electric field vector as a function of $\theta_i$, we have to make use of Snell's law:

$$\sin\theta_t = \frac{\gamma_1}{\gamma_2}\sin\theta_i \tag{2a}$$

$$\cos\theta_t = \sqrt{1-\left(\frac{\gamma_1}{\gamma_2}\right)^2 \sin^2\theta_i} = p \cdot e^{i\cdot\delta} \tag{2b}$$

From the preceding equations and the observation of Figure 1a it is readily seen that the components of the electric field vector into Region 2 can be expressed in the following form:

$$E_x^t = T_{//} \cdot E_o^i \cdot \sin\theta_t \cdot e^{A\cdot(x-x_1)} \cdot e^{-\beta_1 \sin\theta_i \cdot z} \tag{3a}$$

$$E_z^t = T_{//} \cdot E_o^i \cdot \cos\theta_t \cdot e^{A\cdot(x-x_1)} \cdot e^{-\beta_1 \sin\theta_i \cdot z} \tag{3b}$$

where:

$$A = p \cdot (\alpha_2 \cos\delta - \beta_2 \sin\delta) + i \cdot p \cdot (\alpha_2 \sin\delta + \beta_2 \cos\delta) \tag{3c}$$

The components of the EM field vector into region 2 that affect the transmission line are $E_z^t$, $E_x^t$, $H_y^t$ and all of them exist for this particular case. Starting from Faraday's law-expressed in frequency domain-in the surface $\Delta S$ lying in the $x$-$z$ plane bounded by $x = 0,\ x = b,\ z = z,\ z = z + \Delta z$:

$$\oint \vec{E} \cdot d\vec{l} = -j\omega \iint_{\Delta S} \vec{B} \cdot d\vec{S} \tag{3d}$$

and following the mathematical procedure proposed in [1], we can obtain the following system of two uncoupled second-order integro-differential equations (the magnetic field components have been substituted by the relevant electric field ones):

$$\frac{\partial^2}{\partial z^2} V(z) - Y \cdot Z \cdot V(z) = Z^{\text{int}} \cdot Y \int_0^b E_x^t(x,z) \cdot dx \tag{3e}$$

$$\frac{\partial^2}{\partial z^2} I(z) - Y \cdot Z \cdot I(z) = -Y \cdot \left[E_z^t(b,z) - E_z^t(0,z)\right] \tag{3f}$$

(where $Y,\ Z,\ Z^{\text{int}}$ are given in Appendix A).

The equations of the terminal conditions are given:

$$\begin{aligned} V(0) &= -I(0)\cdot R_S \\ V(s) &= I(s)\cdot R_L \end{aligned} \tag{3g}$$

The induced voltages $V_S,\ V_L$ may be obtained [2] from (3e), (3f), (3g):

$$\begin{aligned} V_S &= V(0) = -I(0)\cdot R_S = -\frac{R_s}{D}\cdot I_1 + \frac{R_s\cdot Z_c}{D}\cdot I_2 \\ &\quad -\frac{R_s\cdot(Z_c\cosh\gamma_2 s + R_L\sinh\gamma_2 s)}{D}\cdot I_3 \end{aligned} \tag{4a}$$

$$\begin{aligned} V_L &= V(s) = I(s)\cdot R_L = \frac{R_L}{D}\cdot I_1' + \frac{R_L\cdot Z_c}{D}\cdot I_3 \\ &\quad -\frac{R_L\cdot(Z_c\cosh\gamma_2 s + R_s\sinh\gamma_2 s)}{D}\cdot I_2 \end{aligned} \tag{4b}$$

where

$$\begin{aligned} D &= (Z_c\cdot R_s + R_L\cdot Z_c)\cosh\gamma_2 s + \left(Z_c^2 + R_L\cdot R_s\right)\sinh\gamma_2 s \\ I_1 &= \int_0^s K(z)\cdot[Z_c\cosh\gamma_2(z-s) - R_L\sinh\gamma_2(z-s)]\cdot dz \\ I_1' &= \int_0^s K(z)\cdot[Z_c\cosh\gamma_2 z + R_s\sinh\gamma_2 z]\cdot dz \\ I_2 &= \int_0^b E_x^t(x,s)\cdot dx \\ I_3 &= \int_0^b E_x^t(x,0)\cdot dx \\ K(z) &= E_z^t(b,z) - E_z^t(0,z) \\ Z_C &= \sqrt{Z/Y} \end{aligned}$$

Under the assumption that $R_L = R_S = Z_C$ (conjugate-matched TL), and the evaluation of the integrals defined above, the final relationships for the near- and far-end voltages are expressed:

$$V_s = \frac{1}{2}\cdot T_{//}\cdot E_o^i\cdot e^{-A\cdot x_1}\cdot\left(e^{A\cdot b}-1\right)\cdot\left(e^{-(\gamma_2 + i\cdot\beta_1\cdot\sin\theta_i)\cdot s}-1\right)$$

$$\cdot \left( \frac{p \cdot e^{i\cdot\delta}}{\gamma_2 + i \cdot \beta_1 \cdot \sin\theta_i} + \frac{\gamma_1 \cdot \sin\theta_i}{A \cdot \gamma_2} \right) \tag{5a}$$

$$V_L = \frac{1}{2} \cdot T_{//} \cdot E_o^i \cdot e^{-A\cdot x_1} \cdot \left( e^{A\cdot b} - 1 \right) \cdot \left( e^{-(i\cdot\beta_1\cdot\sin\theta_i)\cdot s} - e^{-\gamma_2\cdot s} \right)$$

$$\cdot \left( \frac{p \cdot e^{i\cdot\delta}}{\gamma_2 - i \cdot \beta_1 \cdot \sin\theta_i} - \frac{\gamma_1 \cdot \sin\theta_i}{A \cdot \gamma_2} \right) \tag{5b}$$

In Figure 1b and 1c, the amplitude and phase of $V_S$ are shown, respectively, with respect to $\theta_i$ for typical parameter values, shown in Table 1.

**Table 1.** Values for the parameters used for numerical evaluation.

| | | |
|---|---|---|
| Resonant frequency | $f$ | 1 GHz |
| Wavenumber | $k$ | $20.94\,\mathrm{m}^{-1}$ |
| Relative permittivity | $\varepsilon_{r2}$ | 50.50 |
| Conductivity | $\sigma_2$ | 1.35 S/m |
| TL depth | $x_1$ | 30 mm |
| TL length | $s$ | 8 mm |
| TL width | $b$ | 2 mm |

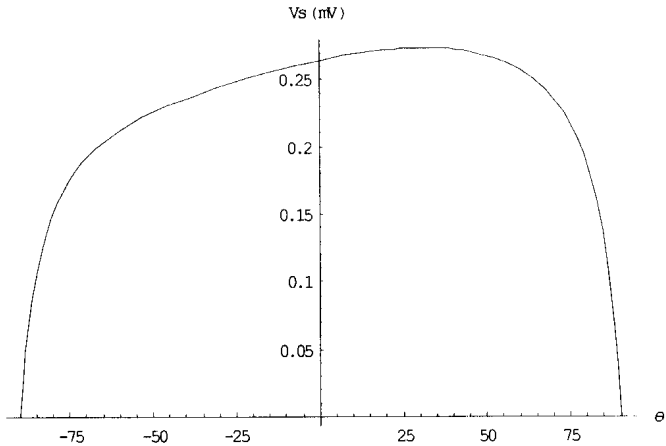


**Figure 1b.** Amplitude of $V_s$ with respect to angle $\theta_i$ (par).

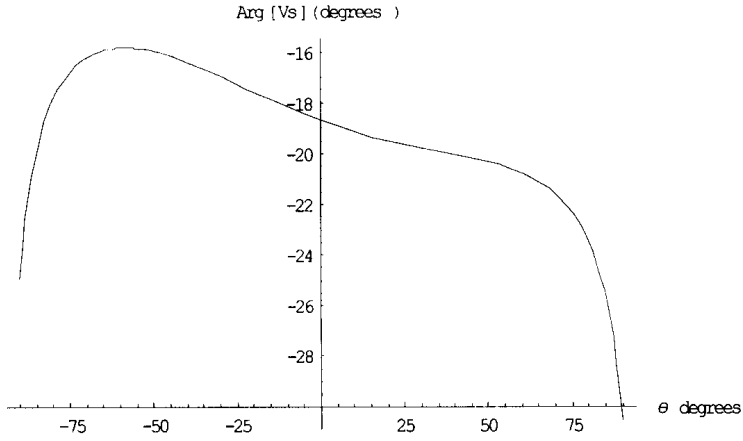


**Figure 1c.** Phase of $V_s$ with respect to angle $\theta_i$ (par).

*Case II (perp1)*
Consider the two Cartesian coordinate systems described in Case I. The incident plane wave at Region 1, is perpendicularly polarized as shown in Figure 2a ($E_y^i,\ H_x^i,\ H_z^i$).

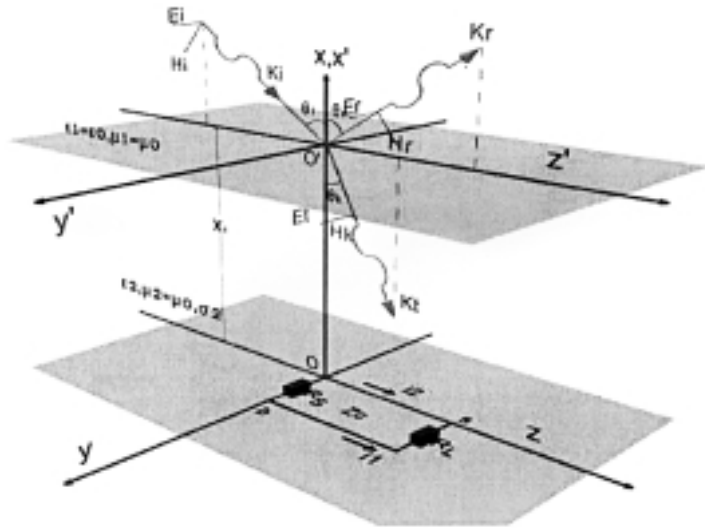


**Figure 2a.** Geometry of Case II (perp1).

The transmission coefficient of the vertically polarized field, corresponding to the interface between Region 1 and 2 is expressed as:

$$T_V = \frac{2 \cdot \gamma_1 \cdot \cos\theta_i}{\gamma_1 \cdot \cos\theta_i + \sqrt{\gamma_2^2 - \gamma_1^2 \cdot \sin^2\theta_i}} \tag{6}$$

The TL is placed at $y$-$z$ plane. It is readily seen that the $z$-component of the magnetic field does not contribute to the line response, according to the specific TL model. On the contrary, $E_y$ and $H_x$ components produce an equivalent current and voltage source, respectively. By analogy with Case I, starting from Faraday's law, it is easy to derive once again the voltage at the near ($z = 0$) and far ($z = s$) end of the TL:

$$V_s = \frac{1}{2} \cdot b \cdot E_o^i \cdot T_V \cdot e^{-A \cdot x_1} \cdot \left( e^{-\gamma_2 \cdot s} \cdot e^{-\gamma_1 \cdot \sin\theta_i s} - 1 \right) \tag{7a}$$

$$V_L = \frac{1}{2} \cdot b \cdot E_o^i \cdot T_V \cdot e^{-A \cdot x_1} \cdot \left( e^{-\gamma_2 \cdot s} - e^{-\gamma_1 \cdot \sin\theta_i s} \right) \tag{7b}$$

In Figures 2b and 2c the amplitude and phase of $V_S$. are shown, respectively for parameter values shown in Table 1.

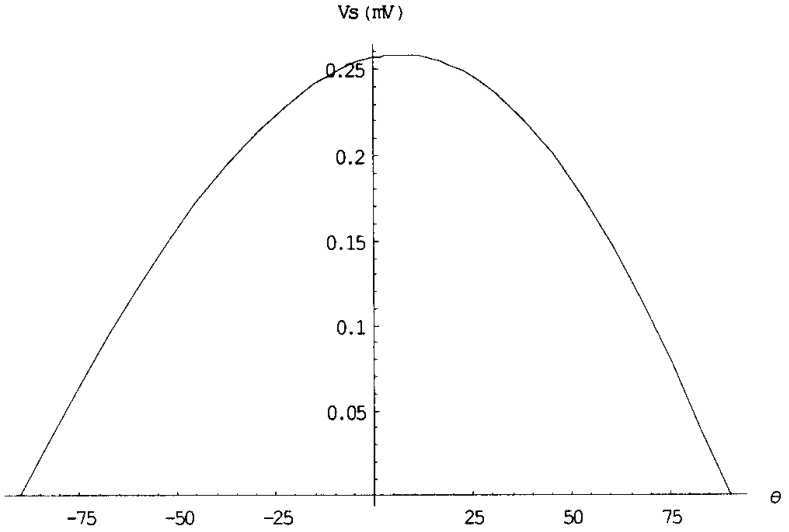


**Figure 2b.** Amplitude of $V_S$ with respect to angle $\theta_i$ (perp1).

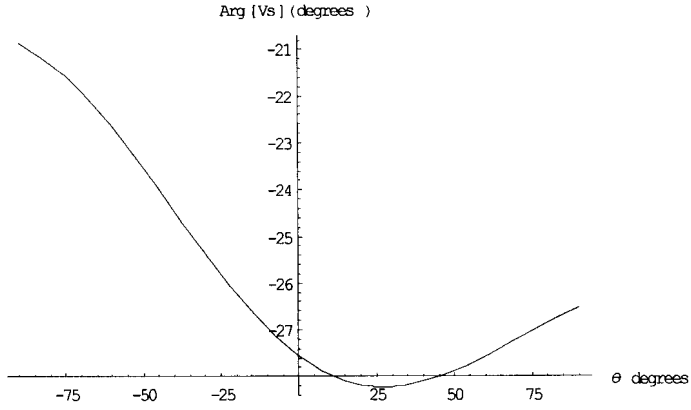


**Figure 2c.** Phase of $V_S$ with respect to angle $\theta_i$ (perp1).

*Case III (perp2)*
In the last case under study, the wave propagates as in the latter case, but the transmission line is turned 90° about $x$-axis, as shown in Figure 3a.

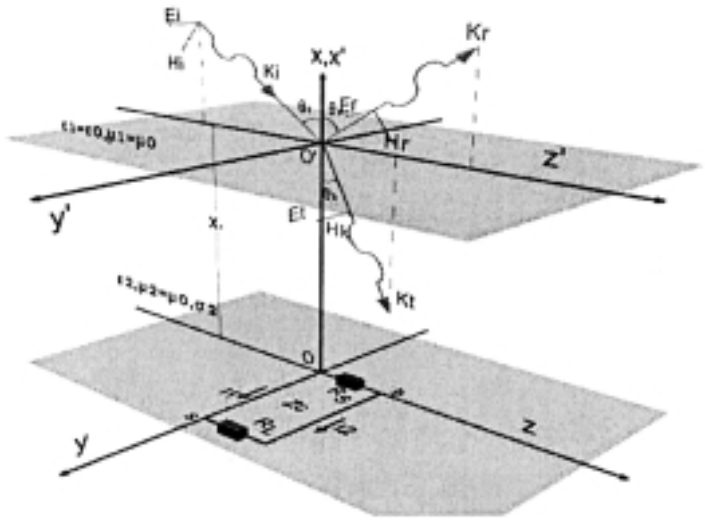


**Figure 3a.** Geometry of Case III (perp2).

The difference from the previously discussed case is that the electric field component is no longer parallel to the near and far end of the line, but to the wires connecting the loads. This small alteration in the configuration can result in a significant increment in the possibility of the induced $V_S$. taking a specific value, different from the other cases as it will be seen in Section 4. Employing the preceding analysis, the induced voltage expressions can be written in the following equations:

$$V_s = -E_o^i \cdot T_V \cdot \frac{i \cdot \gamma_1}{2 \cdot k_0 \cdot \gamma_2^2} \cdot e^{-A \cdot x_1} \cdot \left(e^{-\gamma_1 \sin\theta_i \cdot b} - 1\right) \cdot \left(e^{-\gamma_2 \cdot s} - 1\right) \cdot \left(\frac{\gamma_1^2 \cdot \sin^2\theta_i}{\gamma_2} + A \cdot p \cdot e^{i \cdot \delta}\right) \tag{8a}$$

$$V_L = E_o^i \cdot T_V \cdot \frac{i \cdot \gamma_1}{2 \cdot k_0 \cdot \gamma_2^2} \cdot e^{-A \cdot x_1} \cdot \left(e^{-\gamma_1 \sin\theta_i \cdot b} - 1\right) \cdot \left(e^{-\gamma_2 \cdot s} - 1\right) \cdot \left(\frac{\gamma_1^2 \cdot \sin^2\theta_i}{\gamma_2} + A \cdot p \cdot e^{i \cdot \delta}\right) \tag{8b}$$

where

$$k_0 = \omega\sqrt{\mu_0 \cdot \varepsilon_0}$$

In Figures 3b and 3c, the amplitude and phase of $V_S$. are shown, with respect to the values presented in Table 1.

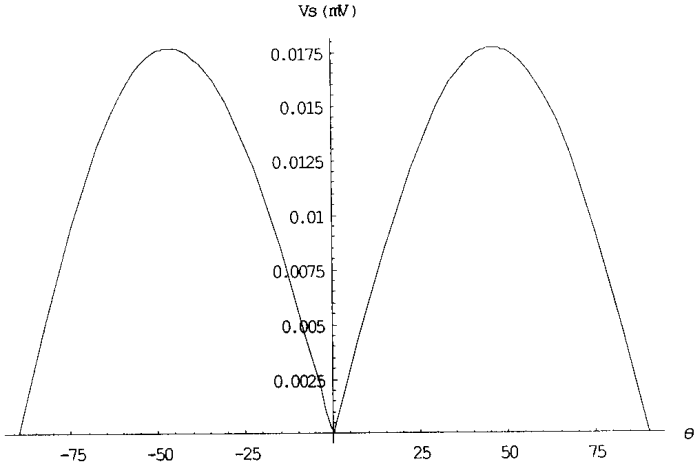


**Figure 3b.** Amplitude of $V_S$ with respect to angle $\theta_i$ (perp2).

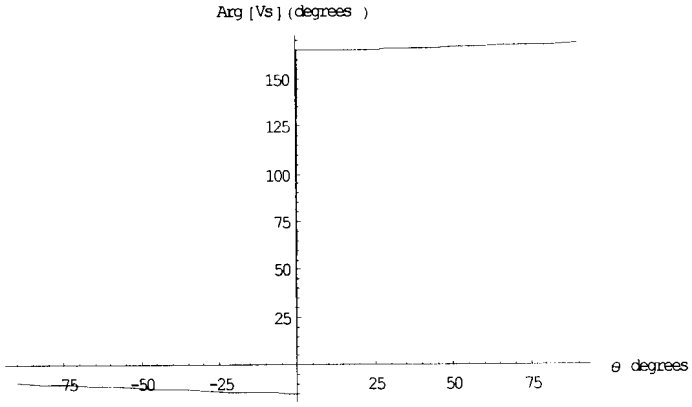


**Figure 3c.** Phase of $V_S$ with respect to angle $\theta_i$ (perp2).

By interpretation of equations (5), (7), (8) as well as from the observation of Figures 1b, 2b, 3b we can conclude that in Cases I and II, the magnitude of $V_S$. is less affected by the angle of incidence, compared to Case III. Moreover, despite Cases I and II, the maximum value of $|V_S|$ in Case III is observed at $\theta_i \cong \pm 50°$. Finally, we notice that the maximum value of $|V_S|$ in Cases I and II is one order larger than the one observed in Case III. This fact occurs due to the absence of the $z$-component contribution of the electric field vector.

## 3. PROBABILISTIC RESULTS FOR THREE GEOMETRIES

Up to this point a deterministic analysis has been discussed for the three cases under study. In this section, the evaluation of the probability density function (pdf) and cumulative distribution function (cdf) of the amplitude of the voltage $V_S$ will be derived for the previously examined cases (see Appendix B for details on probabilistic analysis). Although the expressions of the voltage induced at the far-end of the transmission line are also explicitly introduced above, they will not be examined in this Section. However, the evaluation of $V_L$ can be computed on the same notation as for $V_S$. The amplitude of $V_S$ for the three cases can be written in the general form given below:

$$|V_s| = g\left(E_o^i, \theta_i\right) = E_o^i \cdot |h\left(\theta_i\right)| \tag{9}$$

In many real cases transmission lines are placed inside a dielectric layer which is exposed to the EM field of an antenna radiating in

the far field region. We can imagine situations where the structure (comprised of the dielectric layer and the TL) is randomly moving inside the field. In such cases, the incident field can be modeled as having a Rayleigh distributed amplitude and the angle of incidence is usually uniformly distributed, as reported in [14]. In what follows, these two basic assumptions have been taken into account in order to characterize the statistical behavior of near-end induced voltage $V_S$ with respect to the characteristics of the incident field. The amplitude of the electric field $E_0^i$ propagating in free space is considered to be a random variable with Rayleigh distribution [15]. Furthermore, the angle of incidence is considered to be a uniform variable. These two variables are independent; thus their probability density function can be written as follows [15]:

$$f_{E_o^i}\left(E_o^i\right) = \frac{E_o^i}{v^2} \cdot \exp\left(-\frac{E_o^{i^2}}{2 \cdot v^2}\right), \quad E_o^i \geq 0 \tag{10a}$$

$$f_{\theta_i}\left(\theta_i\right) = \frac{1}{\pi}, \quad -\frac{\pi}{2} \leq \theta_i \leq \frac{\pi}{2} \tag{10b}$$

$$\tag{10c}$$

In order to evaluate the pdf of $V_S$, an auxiliary variable must be properly chosen ($\theta_i$). The joint pdf of $V_S$, $\theta_i$ is expressed [15] as:

$$f_{|V_S|,\theta_i}\left(|V_S|, \theta_i\right) = \frac{1}{\pi} \cdot \frac{f_{E_o^i}\left(\dfrac{|V_S|}{|h\left(\theta_i\right)|}\right)}{|h\left(\theta_i\right)|} \tag{10d}$$

Integrating the latter equation for $\theta_i$, the pdf of $V_S$ arises:

$$f_{|V_S|}\left(|V_S|\right) = \int_{-\pi/2}^{\pi/2} f_{|V_S|,\theta_i}\left(|V_S|, \theta_i\right) \cdot d\theta_i \tag{11}$$

By substituting equations (5a), (7a), (8a) sequentially into (11), we can obtain the pdf of $V_S$ in each case:

$$f_{|V_S|}\left(|V_S|\right) = \frac{1}{\pi} \cdot \int_{-\pi/2}^{\pi/2} \frac{|V_S|}{v^2 |h(\theta_i)|^2} \cdot \exp\left(-\frac{|V_S|^2}{2v^2 |h(\theta_i)|^2}\right) d\theta_i \tag{12}$$

where, for Case I:

$$|h(\theta_i)| = \left|\frac{1}{2} T_{//} e^{-Ax_1} \left(e^{Ab} - 1\right) \left(e^{-(\gamma_2 + \gamma_1 \sin\theta_i)s} - 1\right) \frac{1}{A}\right| \tag{13a}$$

for Case II:

$$|h(\theta_i)| = \left| \frac{b}{2} T_V e^{-Ax_1} \left( e^{-(\gamma_2 + \gamma_1 \sin\theta_i)s} - 1 \right) \right| \tag{13b}$$

and for Case III:

$$|h(\theta_i)| = \left| \frac{1}{2\gamma_2} T_V e^{-Ax_1} \left( e^{-\gamma_2 s} - 1 \right) \left( e^{-(\gamma_1 \sin\theta_i)s} - 1 \right) \right| \tag{13c}$$

The mean value of the amplitude of $V_S$ can be evaluated using the following equation:

$$\begin{aligned} E\left(|V_S|\right) &= \int_0^{+\infty} |V_S| \cdot f_{V_S}\left(|V_S|\right) d\,|V_S| \\ &= \int_{-\pi/2}^{\pi/2} d\theta_i \frac{1}{\pi v^2 \left|h\left(\theta_i\right)\right|^2} \int_0^{+\infty} |V_S|^2 \exp\left( -\frac{|V_S|^2}{2v^2 |h(\theta_i)|^2} \right) d\,|V_S| \\ &= \int_{-\pi/2}^{\pi/2} d\theta_i v \left|h\left(\theta_i\right)\right| \frac{1}{\sqrt{2\pi}} \end{aligned} \tag{14}$$

Equation (14) will be proved very useful for the numerical computation.

## 4. NUMERICAL RESULTS

In this section, what we set out to do is to compute the pdf and cdf of the magnitude of $V_S$ for the three cases under study and explain the differences among them. Equation (12) is the basis for further development of this paper. Integration of (12) brings forward very useful results; for that purpose, appropriate values must be chosen for the dimensions of the transmission line ($s$, $b$), the depth ($x_1$), the conductivity and relative permittivity of region 2($\sigma_2$, $\varepsilon_{r2}$), the resonant frequency of the EM field ($f = c/\lambda$), and finally the parameter $v$ of Rayleigh distribution ($v = 2.4$). Suppose Region 2 as characterized, once again, by the values of Table 1 (see also [13]) and the resonant frequency set equal to 1 GHz. It is of great importance to mention that the value of the Rayleigh distribution parameter, denoted by $v$, has been chosen in such way considering that the mean value of the electric vector in free space is approximately 3 V/m (Appendix B).

In Figures 4, 5 the pdf and cdf of the amplitude of $V_S$ for Case I are shown. The mean value of $V_S$ has been evaluated equal to 0.23 mV and the mean square value equal to 0.071 mV.

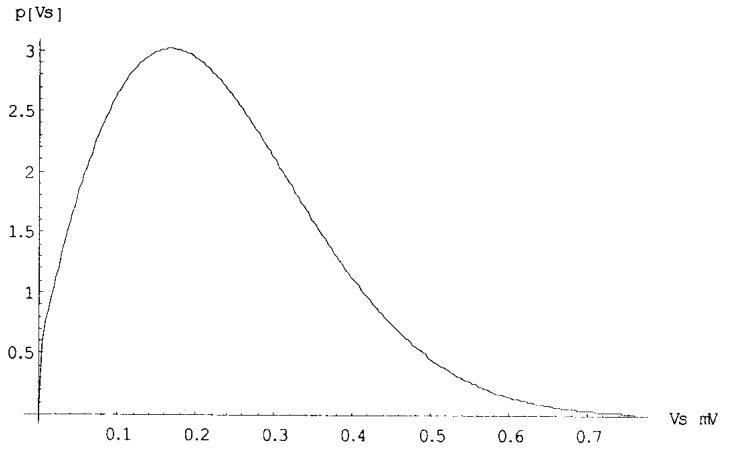


**Figure 4.** Pdf of amplitude of $V_S$ for Case I.

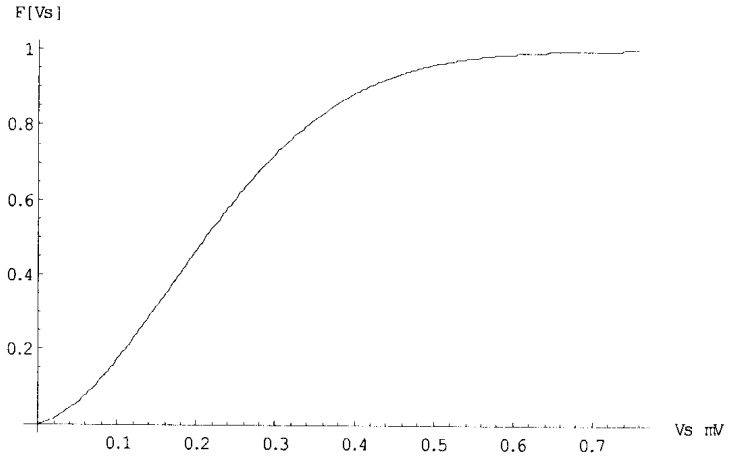


**Figure 5.** Cdf of amplitude of $V_S$ for Case I.

We can observe from Figure 4, that the maximum occurrence probability value for the voltage is 0.17 mV.

In Case II (Figures 6 and 7), the mean value of $V_S$ has been evaluated equal to 0.167 mV and the mean square value equal to 0.043 mV.

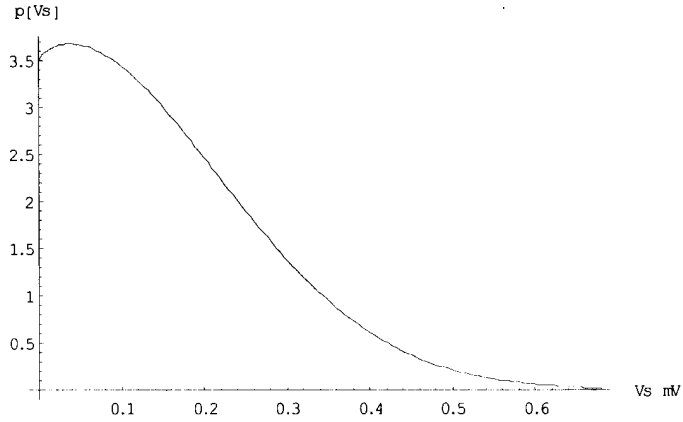


**Figure 6.** Pdf of amplitude of $V_S$ for Case II.

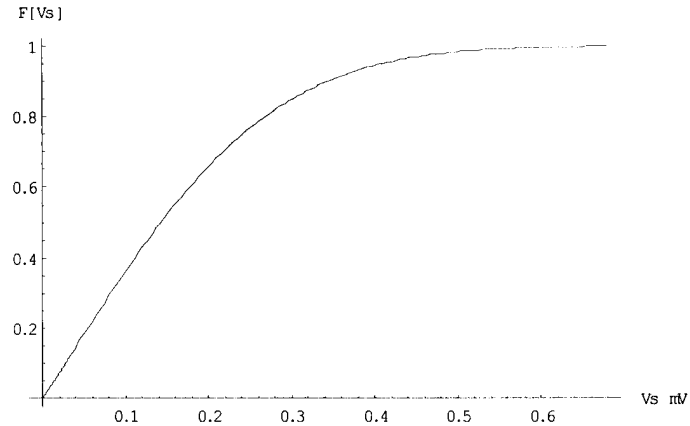


**Figure 7.** Cdf of amplitude of $V_S$ for Case II.

Furthermore, the value of voltage is 0.039 mV, which is much more smaller than the one evaluated in Case I. The critical point is that the value of voltage in Case II is more possible to appear than the one evaluated in Case I.

Finally, in Case III, one can in the same way conclude that the mean value is equal to 0.045 mV and the mean square value is 0.003 mV (Figures 8 and 9). Once again, the values for Case III are smaller than the ones evaluated for Case I, but the appearance probability is much

larger than in Case I. The maximum occurrence probability value of voltage is 0.004 mV.

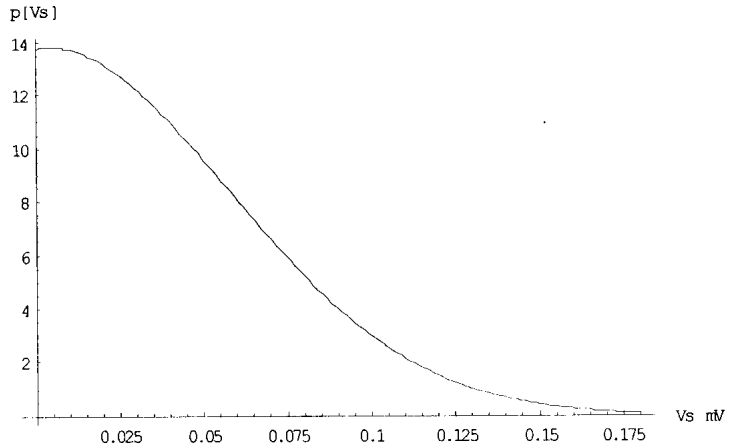


**Figure 8.** Pdf of amplitude of $V_S$ for Case III.

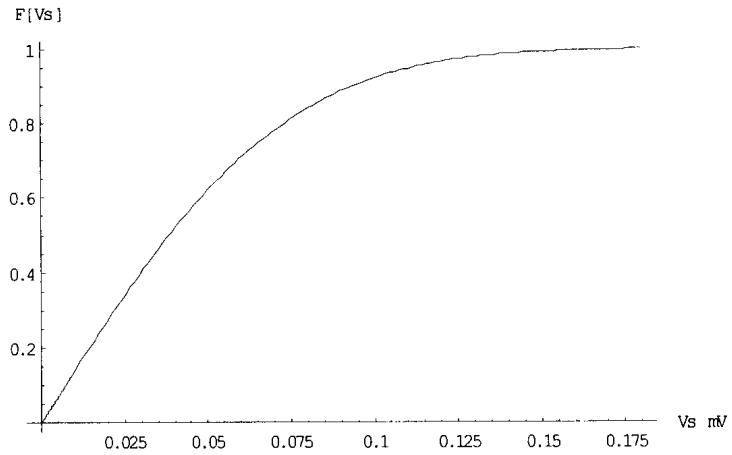


**Figure 9.** Cdf of amplitude of $V_S$ for Case III.

It is important to mention that although it is not obvious from Figures 6, 8, the pdf of the amplitude of $V_S$ in Cases II, III starts from point (0, 0).

The general conclusion coming up from the investigation of the three cases is that in Case I the maximum occurrence probability value of $V_S$ lies between 0.1 and 0.3 mV/m while in Case II the same interval is moved to the left (0.0, 0.2) mV/m and finally in Case III it is obvious that the maximum occurrence probability value of $V_S$ lies in an interval very close to 0 mV/m (e.g., [0.0, 0.075]).

A close look in the previous Figures 4, 6, 8 sets off that the distribution of voltage can be thought as Rayleigh distribution with a different variance from the electric field vector's (Hypothesis $H_0$). A chi-square goodness-of-fit test applied by way of verification. The partition chosen consisted of $m = 25$ segments and the confidence coefficient was set equal to 0.995. From the previously evaluated values of mean and mean square for the three cases, it is obvious that the variance of the distribution under test for each case arises:

$$\begin{aligned} v &= x_{msqv} - (X_{mean})^2 \Rightarrow \\ v_{par} &= 0.183622 \\ v_{perp1} &= 0.133782 \\ v_{perp2} &= 0.036264 \end{aligned} \tag{15}$$

For the test of acceptance of hypothesis $H_0$, the following sum is introduced:

$$q = \sum_{i=1}^{25} \frac{(np_i - np_{0i})^2}{np_{0i}} \tag{16}$$

where: $n = 250$, $p_{0i}$ is the value of the pdf of Rayleigh distribution and $p_i$ is the value of the test distribution.

The evaluation of $q$ [15] for the three cases gives:

$$\begin{aligned} q_1 &= 0.96818, \quad Case\,I \\ q_2 &= 33.8346, \quad Case\,II \\ q_3 &= 36.5924, \quad Case\,III \end{aligned}$$

The value of $\chi^2_{0.995}(24) = 42.9798$, is greater than $q_1$, $q_2$, $q_3$. Consequently, one can accept the hypothesis of Rayleigh distribution for the pdf of the induced voltage for the three cases.

In Figures 10, 11, 12 the curves of $v_{par}/v$, $v_{perp1}/v$, $v_{perp2}/v$ (denoted as $\sigma$) as a function of $\theta_i$ are presented. These figures illustrate the approximate value of parameters $v_{par}$, $v_{perp1}$, $v_{perp2}$ with respect to the incident angle $\theta_i$.

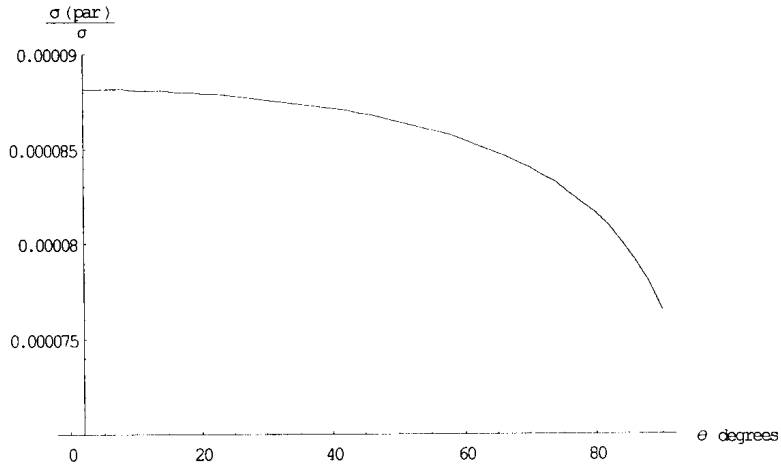


**Figure 10.** Variation of the Rayleigh parameter as a function of angle $\theta_i$ (Case I).

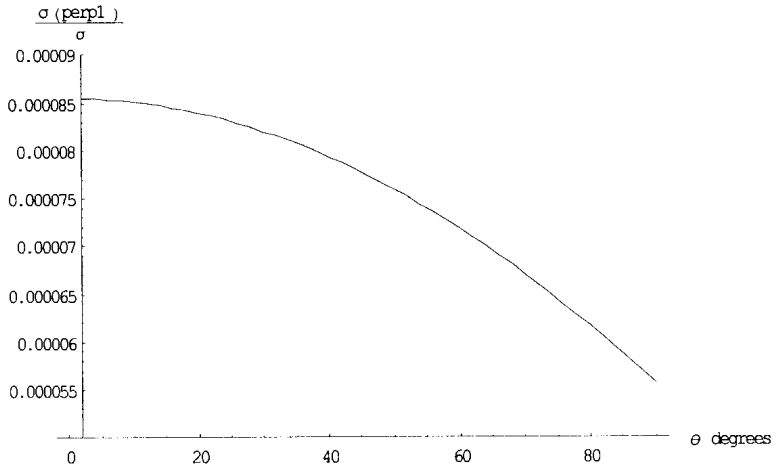


**Figure 11.** Variation of the Rayleigh parameter as a function of angle $\theta_i$ (Case II).

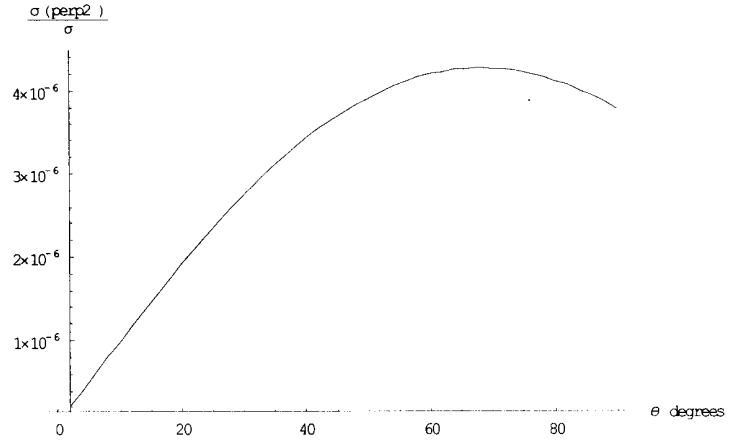


**Figure 12.** Variation of the Rayleigh parameter as a function of angle $\theta_i$ (Case III).

## 5. CONCLUSION

In this paper a statistical analytic model is developed enabling the computation of the induced voltage at the near- and far-end of a TL illuminated by an EM wave propagating in free space. The privilege emerging from the analytic approach of the problem, compared to a brute-force simulation technique is that gives an insight to the nature of the problem. Thus, we can characterize the parameters of significant contribution. Moreover, the solution of the integral in case of the problem is treated analytically is not time-consuming compared to the simulation technique. From the results presented, very useful conclusions arise, such as the worst placement of the transmission line by means of the maximum voltage induced on the near-end termination load and the statistical distribution that the magnitude of the voltage follows; it was proved that the Rayleigh distribution fits well. In addition, curves showing the alteration of approximate variance value of Rayleigh are presented.

## APPENDIX A.

The two propagation constants, appear at the above analysis, consist of a real part that is the attenuation factor denoted as $\alpha_i$ and the imaginary part $\beta_i$ that is the phase factor. The equations giving the

values of each one of them are mentioned:

$$a_1 = 0 \tag{A1}$$

$$a_2 = \omega\sqrt{\frac{\mu_0\varepsilon_2}{2}} \cdot \left[\sqrt{1+\left(\frac{\sigma_2}{\omega\varepsilon_2}\right)^2} - 1\right]^{1/2} \tag{A2}$$

$$\beta_1 = \omega\sqrt{\mu_0\varepsilon_0} \tag{A3}$$

$$\beta_2 = \omega\sqrt{\frac{\mu_0\varepsilon_2}{2}} \cdot \left[\sqrt{1+\left(\frac{\sigma_2}{\omega\varepsilon_2}\right)^2} + 1\right]^{1/2} \tag{A4}$$

Also, the equation giving the distributed series impedance of the transmission line, denoted as $Z$ can be expressed [1] as:

$$Z = 2Z^{\text{int}} + i\omega l^e \tag{A5}$$

where:

$Z^{\text{int}}$ is the internal impedance per-unit-length of the upper and lower wire, and $l^e$ is equal to:

$$l^e = \frac{\mu}{\pi}\ln\left(\frac{b}{a}\right) \tag{A6}$$

where $b$ is the width of the transmission line and $\alpha$ is the conductor radius.

Finally, the distributed shunt admittance of the line conductors, $Y$, is given by:

$$Y = \frac{ik^2}{\omega l^e} \tag{A7}$$

## APPENDIX B.

*Uniform Distribution*

$$f_x(x) = \begin{cases} \dfrac{1}{x_2 - x_1}, & x_1 \le x \le x_2 \\ 0, & \text{elsewhere} \end{cases} \tag{B1}$$

*Rayleigh Distribution*

$$f_x(x) = \begin{cases} \dfrac{x}{v^2} \cdot \exp\left[-\dfrac{x^2}{2v^2}\right], & x > 0 \\ 0, & x \le 0 \end{cases} \tag{B2}$$

*Rayleigh Parameter*
The value of parameter $v$ of the Rayleigh distribution that the electric field vector follows (random variable) was set equal to 2.4. This value appears if we get the mean value of the distribution equal to 3 V/m. The equation giving variance as a function of mean value is:

$$\bar{x} = \sqrt{\frac{\pi}{2}} \cdot v \Rightarrow v = \sqrt{\frac{2}{\pi}} \cdot \bar{x} = 2.4\,\mathrm{V/m} \tag{B3}$$

*Variable Transformation*
Suppose that $\mathbf{x}$ is a continuous, real, random variable and $g(x)$ is a function of $x$. The expression $y = g(x)$ is a new random variable; then

$$f_y(y) = \frac{f_x(x_1)}{|g'(x_1)|} + \frac{f_x(x_2)}{|g'(x_2)|} + \cdots + \frac{f_x(x_m)}{|g'(x_m)|} \tag{B4}$$

where $g'(x)$ is the derivative of $g(x)$.

In the case of two variables, the previous equation becomes:

$$f_{z,w}(z,w) = \frac{f_{x,y}(x_1,y_1)}{|J(x_1,y_1)|} + \cdots + \frac{f_{x,y}(x_m,y_m)}{|J(x_m,y_m)|} \tag{B5}$$

where $(x_i, y_i),\ \forall i \in [1,m]$ are the real roots of equations $g(x_i,y_i) = z,\ h(x_i,y_i) = w$, and

$$J(x,y) = \begin{vmatrix} \dfrac{\partial z}{\partial x} & \dfrac{\partial z}{\partial y} \\ \dfrac{\partial w}{\partial x} & \dfrac{\partial w}{\partial y} \end{vmatrix} \tag{B6}$$

*Hypothesis Test*
The chi-square test is used in goodness-of-fit tests involving the agreement between experimental data and theoretical models. We are given a partition $A = [A_1, A_2, \cdots, A_m]$ of the space $S$ and we wish to test the hypothesis:

$$H_0 : p_i = p_{0i},\ \text{all } i \quad \text{against} \quad H_1 : p_i \neq p_{0i},\ \text{some } i \tag{B7}$$

using as data the number of successes $k_i$ of each of the events $A_i$ in $n$ trials. For this purpose, we introduce the sum

$$q = \sum_{i=1}^{m} \frac{(k_i - n \cdot p_{0i})^2}{n \cdot p_{0i}} \tag{B8}$$

From equation (B17) we can compute $q$; also we can find the value of $\chi^2_{1-a}(m-1)$ from well known tables [14]. If

$$q < \chi^2_{1-a}(m-1) \tag{B9}$$

then hypothesis $H_0$ is accepted.

## REFERENCES


1. Taylor, C. D., R. S. Satterwhite, and C. W. Harrison, Jr., "The response of a terminated two-wire transmission line excited by a nonuniform electromagnetic field," *IEEE Trans. Antennas Prop. (Commun.),* Vol. AP-13, No. 11, 987–989, Nov. 1965.
2. Smith, A. A. Jr., "A more convenient form of the equations for the response of a transmission line excited by nonuniform fields," *IEEE Trans. on EMC (Correspondence),* Vol. 19, No. 3, 151–152, 1973.
3. King, R. W. P. and C. W. Harrison, Jr., "Excitation of an external terminated longitudinal conductor on a rocket by a transverse electromagnetic field," *IEEE Trans. on EMC,* Vol. EMC-14, No. 1, 1–3, 1972.
4. Harrison, C. W. Jr., "Bounds on the load currents of exposed one- and two-conductor transmission lines electromagnetically coupled to a rocket," *IEEE Trans. on EMC,* Vol. EMC-14, No. 1, 4–9, 1972.
5. Bechtold, G. W. and D. J. Kozakoff, "Transmission line response of a multiconductor cable in a transient electromagnetic field," *IEEE Trans. on EMC,* Vol. EMC-12, No. 1, 5–8, 1970.
6. Ari, N. and W. Blumer, "Analytic formulation of the response of a two-wire transmission line excited by a plane wave," *IEEE Trans. on EMC,* Vol. 30, No. 4, 437–448, 1988.
7. Bridges, G. E., "Transient plane wave coupling to bare and insulated cables buried in a lossy half-space," *IEEE Trans. on EMC,* Vol. 37, No. 1, 62–70, 1995.
8. Shiran, S., B. Reiser, and H. Cory, "A probabilistic model for the evaluation of coupling between transmission lines," *IEEE Trans. on EMC,* Vol. 35, No. 3, 387–393, 1993.
9. Nucci, C. A. and F. Rachidi, "On the contribution of the electromagnetic field components in field-to-transmission line interaction," *IEEE Trans. on EMC,* Vol. 37, No. 4, 505–508, 1995.
10. Cooray, V., "Calculating lightning-induced overvoltages in power lines: a comparison of two coupling models," *IEEE Trans. on EMC,* Vol. 36, No. 3, 1994.

11. Nucci, C. A., et al., "Comparison of two coupling models for lightning-induced overvoltage calculations," presented in *IEEE PES Summer Meeting,* Vancouver, BC, Canada, 1993.
12. Balanis, C. A., *Advanced Engineering Electromagnetics,* John Wiley & Sons, 1989.
13. King, R. W. P. and G. S. Smith, *Antennas in Matter,* MIT Press, 1981.
14. Rappaport, T. S., *Wireless Communications,* Chapter 4, Prentice Hall PTR, 1996.
15. Papoulis, A., *Probability, Random Variables and Stochastic Processes,* McGraw-Hill, New York, 1981.
16. Capraro, G. T. and C. R. Paul, "A probabilistic approach to wire coupling interference prediction," Proc. 4th *International Zurich Symposium on EMC,* 267–272, Zurich 1981.
17. Weiner, D. and G. T. Capraro, "A statistical approach to EMI theory and experiment," Proc. 7th *International Zurich Symposium on EMC,* 629–633, Zurich 1987.
18. Holland, R. and R. H. St. John, "Statistical response of EM-driven cables inside an overmoded enclosure," *IEEE Trans. on EMC,* Vol. 40, No. 4, 311–324, 1998.
19. Bellan, D. and S. Pignari, "A probabilistic model for the transmission line voltages induced by an external field," Proc. 15th *International Wroclaw Symposium on EMC,* June 2000.
20. Bellan, D. and S. Pignari, "A probabilistic model for a three-conductor transmission line driven by random plane wave field," Proc. 4th *International Symposium on EMC,* EMC Europe 2000, Brugge, September 2000.